2023 31st Mediterranean Conference on Control and Automation (MED)
June 26 - 29, 2023. Limassol, Cyprus

2023 31st Mediterranean Conference on Control and Automation (MED) | 979-8-3503-1543-1/23/$31.00 ©2023 IEEE | DOI: 10.1109/MED59994.2023.10185864

Fundamental Limits on Disturbance Propagation in Virtual Viscoelastic-based Multi-Agent Systems

Dinesh Murugan, Rozhin Hajian, and Milad Siami

***Abstract*— In this paper, we investigate the performance deterioration of commensurate fractional-order consensus networks under exogenous stochastic disturbances. We formulate fractional-order differential equations for the network dynamics using Caputo derivatives and the Laplace transform, and employ the $\mathcal{H}_2$ norm of the dynamical system as a performance measure. By developing a graph-theoretic methodology, we relate the structural specifications of the underlying graphs to the performance measure and explicitly quantify fundamental limits on the best achievable levels of performance in fractional-order consensus networks. We also establish new connections between the sparsity of the network and the performance measure, characterizing fundamental tradeoffs that reveal the interplay between the two. Finally, we provide numerical illustrations to verify our theoretical results, which could help in the design of robust fractional-order control systems in the presence of disturbances.**

I. Introduction

Background: The study of complex dynamical networks has been a subject of growing interest in recent years, with a focus on the accurate description and modeling of such systems [1]–[4]. While many canonical models and methods exist, complex systems still have eluded quantitative analytic descriptions. One such example is soft/flexible robots, which are entailed by elastic properties that ordinary differential equations cannot fully capture [5]–[8]. *Fractional-order systems* have been proposed as a method to model these systems accurately with fewer parameters [9]. Fractional-order systems are considered as an extension of integer order systems, where the state space representation of the dynamic system involves non-integer derivatives of states [10]–[12]. Although there has been considerable research in the field of fractional order systems, limited attention has been given to investigating the robustness of the performance measure of a Fractional-Order Linear Time-Invariant (FLTI) system over various types of underlying graphs.

Objectives and research questions: The role of aggregation in multi-agent systems is crucial for executing complex tasks, such as coordinating the movements of a group of mobile robots to maintain a predetermined formation pattern while sustaining stability in the presence of external disturbances or shocks [13]–[16]. To explore this behavior, this study aims to propose a novel virtual viscoelastic-based model for inter-agent interaction [11]. This model characterizes the sensing abilities of each agent through virtual viscoelastic links, collectively referred to as the Voigt system, which allows each agent to compute its neighbors' states using only local information.

Each robot in the multi-agent system is equipped with sensors and actuators that gather information about the environment and its relative position with respect to other robots. The collected data is then aggregated to determine the desired formation pattern and velocity for the entire team, which is used by each robot to adjust its movements and maintain the predetermined formation pattern, even under adverse conditions such as external disturbances or shocks. The virtual viscoelastic-based model further improves the performance of the system by leveraging fractional-order systems to accurately model the complexities of viscoelastic materials. This results in a more robust and efficient method for modeling and optimizing complex multi-agent networks compared to traditional approaches.

The study aims to answer the following research questions:

- How can virtual viscoelastic models be used to accurately model the behavior of multi-agent systems?
- What is the impact of structural specifications of the underlying graphs of the network on the performance measure?
- What are the trade-offs between sparsity, dynamic complexity, and performance in fractional-order linear consensus networks?
- What is the performance of the proposed virtual viscoelastic-based model for a soft robot, and how does it compare to traditional approaches?

Significance and contribution: The proposed virtual viscoelastic-based model is a significant contribution to the analysis and modeling of multi-agent networks, particularly for systems with long memory and nonlinear interactions. The study integrates control theory, fluid dynamics, network science, and fractional-order calculus to provide a comprehensive analysis of the design of complex soft robots. The findings of this study will have important implications for the design and control of multi-agent systems and will contribute to the development of more efficient and robust methods for modeling and optimizing complex networks.

This research was supported in part by grants ONR N00014-21-1-2431, NSF 2121121, and the Army Research Laboratory and accomplished under Cooperative Agreement Number W911NF-22-2-0001. The views and conclusions contained in this document are those of the authors and should not be interpreted as representing the official policies, either expressed or implied, of the Army Research Office or the U.S. Government.

M. Siami and Dinesh Murugan are with Electrical & Computer Engineering Department, Northeastern University, Boston, MA 02115 USA (e-mails: {m.siami, murugan.di}@northeastern.edu).

R. Hajian is with the Department of Mechanical Engineering, UMass Lowell, MA 01854 USA (e-mail: rozhin_hajian@uml.edu)

Methodology: This paper builds upon previous work on fractional-order systems [17]–[20] and investigates commensurate fractional-order consensus networks. A framework for robustness analysis of commensurate first-order and second-order linear consensus networks is presented, and the performance measure of the system is evaluated using the $\mathcal{H}_2$ norm. The relationship between the performance measure and the underlying graph of the network is explored using a graph-theoretic methodology. The study also highlights the tradeoffs between sparsity, dynamic complexity, and performance in fractional-order linear consensus networks. The proposed methodology is evaluated using numerical illustrations, demonstrating the robustness of fractional-order linear consensus networks under external stochastic disturbances. Finally, the potential of the proposed methodology for designing robust fractional-order control systems in the presence of disturbances is showcased by modeling a fractional-order system for a soft robot. The study represents a significant advancement in the analysis and modeling of multi-agent networks, particularly for systems with long memory and nonlinear interactions.

In this conference paper, the proofs are omitted due to the space limitation.

II. Notations, Definitions, and Basic Concepts

A. Spectral Graph Theory

Let $\mathcal{G} = (\mathcal{V}, \mathcal{E}, w)$, denote an un-directed graph, where $\mathcal{V}$ is the set of nodes, $\mathcal{E} \subseteq \big\{\{i,j\} \bigm| i,j \in \mathcal{V},\ i \neq j\big\}$ is the set of edges, and $w : \mathcal{E} \to \mathbb{R}_{++}$ is the weight function. An unweighted graph $\mathcal{G}$ is a graph with weight function $w(e) = 1$ for $e \in \mathcal{E}$. The adjacency matrix $A = [a_{ij}]$ of graph $\mathcal{G}$ is defined by setting $a_{ij} = w(e)$ if $e = (i,j) \in \mathcal{E}$ and 0 otherwise. The Laplacian matrix L of graph $\mathcal{G} = (\mathcal{V}, \mathcal{E}, w)$ is defined by: $L = \Delta - A$ where $\Delta = \operatorname{diag}[d_1, \cdots, d_n]$, where d_i is the degree of node i. For an undirected and connected graph, the Laplacian matrix L has $n-1$ strictly positive eigenvalues and one zero eigenvalue. The eigenvalues are arranged in the ascending order as $0 = \lambda_1 < \lambda_2 \leq \ldots \leq \lambda_n$. Moreover, the oriented incidence matrix of graph $\mathcal{G}$ is denoted by D. Throughout this paper, a complete graph is represented by $\mathcal{K}_n$, a tree graph is represented by $\mathcal{T}$, a star graph is represented by $\mathcal{S}_n$, and a bipartite graph is represented by $\mathcal{B}_{n1,n2}$.

B. Fractional Calculus

In this work, we concentrate on the Caputo definition of fractional calculus. The definition is expressed mathematically as follows:

$$\frac{d^\alpha}{dt^\alpha} f(t) = \frac{1}{\Gamma(n-\alpha)} \int_0^t (t-\tau)^{n-\alpha-1} \frac{d^n}{dt^n} f(\tau) d\tau, \qquad (1)$$

where α is a positive real number, $\Gamma(.)$ is the Gamma function and n is the first integer not less than α (*i.e.*, $\lceil \alpha \rceil = n$). A Fractional-order Linear Time Invariant (FLTI) system can be represented by the following pseudo state space form

$$\begin{cases} \frac{d^{\bar{\alpha}}}{dt^{\bar{\alpha}}} x(t) \ = \ Ax(t) \ + \ B\xi(t), \\ y(t) \ = \ Cx(t), \end{cases} \qquad (2)$$

where $x \in \mathbb{R}^n$, $u \in \mathbb{R}^m$, $y \in \mathbb{R}^p$, $A \in \mathbb{R}^{n\times n}$, $B \in \mathbb{R}^{n\times m}$, $C \in \mathbb{R}^{p\times n}$, and $\frac{d^{\bar{\alpha}}}{dt^{\bar{\alpha}}}$ refers to the Caputo derivative where $\bar{\alpha} = [\alpha_1 \cdots \alpha_n]^\top$ indicates fractional order settled in the range $(0,2)^n$.

Definition 1: The Mittag Leffler function is defined as follows:

$$E_{\alpha,\beta}(z) = \sum_{k=0}^{\infty} \frac{z^k}{\Gamma(\alpha k + \beta)} \quad \beta > 0,\ \alpha > 0 \qquad (3)$$

where $\Gamma(x)$ is the Gamma function and α and β refers to the fractional order of the system.

III. Robustness Analysis of FLTI Consensus Networks

In this section, we consider the class of linear fractional-order dynamical networks that consist of multiple agents with scalar state variables x_i and control inputs u_i whose dynamics evolve in time according to

$$\frac{d^\alpha}{dt^\alpha} x_i(t) \ = \ u_i(t) + \xi_i(t) \qquad (4)$$

$$y_i(t) \ = \ x_i(t) - \bar{x}(t) \qquad (5)$$

for all $i = 1, \ldots, n$, where $x_i(0) = x_i^*$ is the initial condition and

$$\bar{x}(t) = \frac{1}{n}\big(x_1(t) + \ldots + x_n(t)\big)$$

is the average of all states at time t. The impact of the uncertain environment on each agent's dynamics is modeled by the exogenous anomalous disturbance input $\xi_i(t)$. A virtual viscoelastic-based model for inter-agent interaction is utilized in this study to accurately model multi-agent systems with reduced parameters. This model accounts for long memory and nonlinear interactions between agents, which are modeled through a feedback control law applied to the agents of the network as follows

$$u_i(t) \ = \ \sum_{j=1}^{n} k_{ij}\big(x_j(t) - x_i(t)\big), \qquad (6)$$

the resulting closed-loop system will be a fractional-order linear consensus network. The control law incorporates the virtual viscoelastic inter-agent interaction, which allows for effective capture of the damping properties of agents and is well-suited for modeling real-world multi-agent systems. This approach is based on fractional-order systems, which have been proposed as a method to accurately model the complexities of viscoelastic materials with fewer parameters, offering significant advantages over traditional integer-order models. By utilizing this approach, we can gain insights into the impact of network topology on the performance of fractional-order consensus networks under exogenous stochastic disturbances. The closed-loop dynamics of the network (4)-(5) with feedback control law (6) can be written in the following compact form

$$\Sigma: \begin{cases} \frac{d^\alpha}{dt^\alpha} x(t) = -L\, x(t) \ + \ \xi(t) \\ y(t) = M_n\, x(t), \end{cases} \quad (7)$$

with initial condition $x(0) = x^*$, where $x = [x_1, \ldots, x_n]^\top$ is the state, $y = [y_1, \ldots, y_n]^\top$ is the output, and $\xi = [\xi_1, \ldots, \xi_n]^\top$ is the anomalous disturbance input of the network. The state matrix of the network is a graph Laplacian matrix that is defined by $L = [l_{ij}]$, where

$$l_{ij} := \begin{cases} -k_{ij} & \text{if} \quad i \neq j \\ k_{i1} + \ldots + k_{in} & \text{if} \quad i = j \end{cases} \quad (8)$$

and the output matrix is a centering matrix that is defined by

$$M_n \ := \ I_n - \frac{1}{n} J_n. \quad (9)$$

The underlying coupling graph of the consensus network (7) is a graph $\mathcal{G} = (\mathcal{V}, \mathcal{E}, w)$ with node set $\mathcal{V} = \{1, \ldots, n\}$, edge set

$$\mathcal{E} = \Big\{ \{i, j\} \ \big| \ \forall\, i, j \in \mathcal{V}, \ k_{ij} \neq 0 \Big\}, \quad (10)$$

and weight function $w(e) = k_{ij}$ for all $e = \{i, j\} \in \mathcal{E}$, and $w(e) = 0$ if $e \notin \mathcal{E}$. The Laplacian matrix of graph $\mathcal{G}$ is equal to L.

Assumption 1: The coupling graph $\mathcal{G}$ of the consensus network (7) is connected and time-invariant. Moreover, all feedback gains (weights) satisfy the following properties for all $i, j \in \mathcal{V}$:

(a) non-negativity: $k_{ij} \geq 0$,
(b) symmetry: $k_{ij} = k_{ji}$,
(c) simpleness: $k_{ii} = 0$.

Property (b) implies that feedback gains are symmetric and (c) means that there is no self-feedback loop in the network.

According to Assumption 1, the underlying coupling graph is undirected, connected, and simple. Assumption 1 implies that only one of the modes of network (7) is marginally stable with eigenvector $\mathbf{1}_n$ and all other ones are stable (see [17]). The marginally stable mode, which corresponds to the only zero Laplacian eigenvalue of L, is unobservable from the output (7). The reason is that the output matrix of the network satisfies $M_n \mathbf{1}_n = 0$.

Corollary 1: Assume that there is no exogenous noise input, *i.e.*, $\xi(t) = 0$ for all time, and Assumption 1 holds, then the states of all agents converge to a consensus state, which for network Γ (7), the consensus state is

$$\lim_{t \to \infty} x(t) \ = \ \bar{x}(0) \mathbf{1}_n \ = \ \frac{1}{n} \mathbf{1}_n \mathbf{1}_n^\top \ x^*, \quad (11)$$

Remark 1: For the case of $\alpha = 1$, the result of Corollary 1 recovers the well-known result of ordinary consensus problems [14].

A. Robustness Measure

In order to find the robustness performance of the system, we utilize the frequency domain definition of the (squared) $\mathcal{H}_2$ norm of the system, i.e,

$$\rho(\Sigma, \alpha) := \frac{1}{2\pi} \operatorname{Tr} \left[\int_{-\infty}^{+\infty} G^H(j\omega) G(j\omega) d\omega \right] \quad (12)$$

with transfer matrix:

$$G(s) = M_n (s^\alpha I_n + L)^{-1}. \quad (13)$$

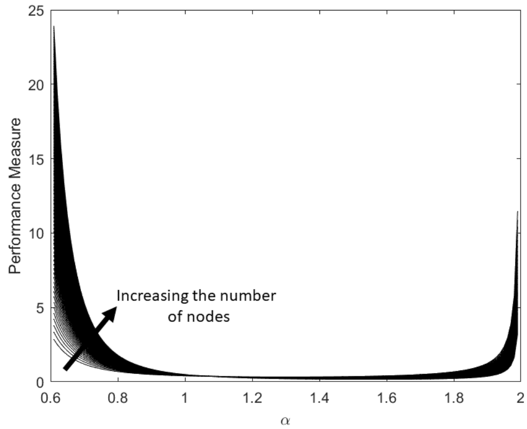

Fig. 1: Performance of a FOC system on a complete graph $\mathcal{G} = \mathcal{K}_n$ as α ranges from 0.5 to 2 and network size (n) from 5 to 1000.

Theorem 1 ([17]): Suppose that an FLTI consensus network (7) over graph $\mathcal{G}$ is given. The performance measure (12) for $\frac{1}{2} < \alpha < 2$ is given by

$$\rho(\Sigma, \alpha) \ = \ \left| \frac{\cot(\frac{\alpha\pi}{2})}{\alpha \sin(\frac{\pi}{\alpha})} \right| \sum_{i=2}^{n} \lambda_i^{-\beta}, \quad (14)$$

where $\beta = 2 - \alpha^{-1}$. Moreover, for $\alpha = 1$, this reduces to

$$\rho(\Sigma, 1) \ = \ \frac{1}{2} \sum_{i=2}^{n} \lambda_i^{-1}.$$

B. Convexity of the Robustness Performance Measure: Implications for Optimization

In this section, we demonstrate that the performance measure of the network over $\mathcal{G}$ exhibits convexity properties with respect to both the eigenvalues λ_i and the fractional-order parameter α.

Formally, we prove that the performance measure of the FLTI network (7) with graph $\mathcal{G}$ is convex with respect to both the eigenvalues λ_i and the fractional-order parameter α.

Lemma 1: The performance measure of the fractional-order LTI consensus network $\rho(\Sigma, \alpha)$ is convex on λ_i, the eigenvalues of the graph, if and only if $\alpha > 0.5$.

Lemma 2: The performance measure of FLTI consensus network (7), denoted by $\rho(\Sigma, \alpha)$, is convex with respect to α if and only if α belongs to the interval $(0.5, 2)$.

The convexity property of the robustness measure (12) is particularly advantageous in optimization problems as it simplifies finding optimal values for the eigenvalues or the fractional-order parameter that minimize performance degradation.

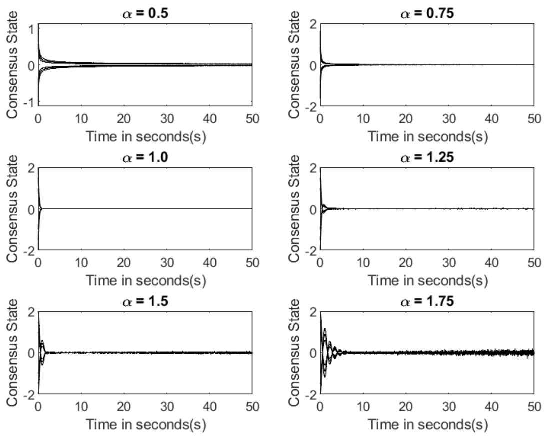

Fig. 2: This plot depicts the consensus states reached by FLTI network consisting of 6 nodes where the underlying graph is a complete graph, $\mathcal{G} = \mathcal{K}_n$, and $\alpha \in (0.5, 2)$ and a Gaussian noise $\mathcal{N}(0, 0.01)$ is being applied to the system.

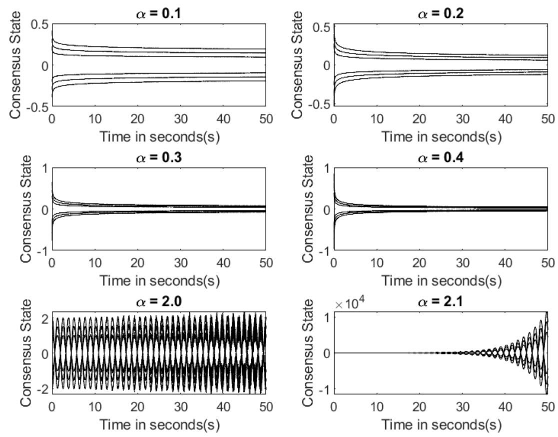

Fig. 3: This plot depicts the consensus states reached by FLTI network consisting of 6 nodes where the underlying graph is a complete graph, $\mathcal{G} = \mathcal{K}_n$, and for $0 < \alpha < 0.5$ and for $\alpha > 2$ and a Gaussian noise $\mathcal{N}(0, 0.01)$ is being applied to the system.

Example 1: Consider a fractional order consensus network (7) consisting of 6 nodes and the underlying graph, connecting them is a complete graph $\mathcal{G} = \mathcal{K}_n$. The value of α ranges from 0 and 2. The network is then stimulated for all the nodes to reach a consensus state. The consensus state depends on the initial conditions of all the nodes. In this example, the nodes are started from an initial position of [-3,-2,-1,1,2,3] respectively. We can see from Fig. 2 and 3, that for $\alpha < 0.5$, and for $\alpha > 2$ the network does not seem to reach a consensus state whereas for $\alpha \in (0.5, 2)$, the network does seem to reach a consensus state. This helps tell that the network is convex in α, when $\alpha \in (0.5, 2)$.

Additionally, Fig. 1 depicts a plot of performance measure against α, for a complete graph, $\mathcal{K}_n$, while simultaneously increasing the number of nodes. We can observe that as $\alpha \to 0.5$ and $\alpha \to 2$, the performance measure of the graph (14) increases, and tries to remain constant while in between.

IV. Scaling Laws for various FLTI Networks

The following result presents the universal lower and upper bounds for the best and the worst achievable values for the performance measure among all fractional order networks with arbitrary unweighted coupling graphs.

Corollary 2: For a given Fractional Order Network with an unweighted coupling graph, $\mathcal{G} \in \mathcal{G}_n$, the performance measure is universally bounded by:

$$n^{-\beta}\ (n-1)\ \le\ \frac{\rho(\Sigma,\alpha)}{\mathfrak{A}}\ \le\ 2^{-\beta}\sum_{k=1}^{n-1}\left(1-\cos(\frac{\pi k}{n})\right)^{-\beta} \quad (15)$$

where $\mathfrak{A} = |\frac{\cot(\frac{\alpha\pi}{2})}{\alpha \sin\frac{\pi}{\alpha}}|$, and $\beta = 2 - \alpha^{-1}$. Moreover, the upper bound is achieved if and only if $\mathcal{G} = \mathcal{P}_n$, i.e., for a path graph, and the lower bound is achieved if and only if $\mathcal{G} = \mathcal{K}_n$, i.e., for a complete graph.

These bounds can be tightened if we consider more specific sub-classes of graphs. In the following theorems, we can improve the bounds by considering various sub-classes of graphs such as tree, and bipartite graphs.

A. Tree Graphs

A tree graph is a connected acyclic un-directed graph in which every node is connected by a single edge. The number of edges present in a complete graph $= n-1$. The maximum degree for a tree graph ranges from 2 to $n-1$.

Corollary 3: For a given fractional order network, with an unweighted tree coupling graph $\mathcal{T} \in \mathcal{G}_n$, with $n \ge 5$, the performance measure is bounded by:

$$(n^{-\beta} + (n-2)^{-\beta-1} \le \frac{\rho(\Sigma,\alpha)}{\mathfrak{A}} \le \le 2^{-\beta}\sum_{k=1}^{n-1}\left(1-\cos(\frac{\pi k}{n})\right)^{-\beta}, \quad (16)$$

where $\mathfrak{A}$ $\left|\frac{\cot(\frac{\alpha\pi}{2})}{\alpha \sin\frac{\pi}{\alpha}}\right|$, and $\beta = 2 - \alpha^{-1}$.

The lower bound is achieved if and only if $\mathcal{T} = \mathcal{S}_n$, and the upper bound is achieved if and only if $\mathcal{T} = \mathcal{P}_n$.

B. Bi-Partite Graphs

Corollary 4: For a given fractional order network, with an unweighted bipartite coupling graph $\mathcal{B}_{n1,n2} \in \mathcal{G}_n$, with $n \ge 5$, the performance measure is bounded by:

$$\left(2.\sqrt{\frac{\mathbf{Z(G)}}{n}}\right)^{-\beta} + \frac{\left(2.m - 2.\sqrt{\frac{\mathbf{Z(G)}}{n}}\right)^{-\beta}}{(n-2)^{-\beta-1}} \le \frac{\rho(\Gamma,\alpha)}{\mathfrak{A}} \le 2^{-\beta}\sum_{k=1}^{n-1}\left(1-\cos(\frac{\pi k}{n})\right)^{-\beta}, \quad (17)$$

where $\mathfrak{A}$ $\left|\frac{\cot(\frac{\alpha\pi}{2})}{\alpha \sin\frac{\pi}{\alpha}}\right|$, and $\beta = \alpha^{-1} - 2$, m is the number of edges, and $\mathbf{Z(G)}$ is the sum of squares of degrees of all the vertex in a graph.

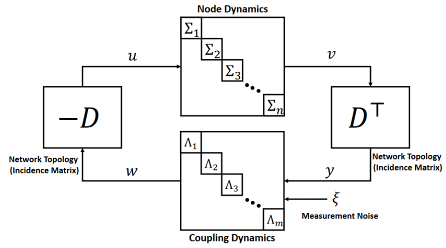

Fig. 4: A block diagram for a Fractional Model System network. Λ_i are fractional-order dynamics (springpot model) and Σ_i are second-order dynamics (mass model). Matrix D is an oriented incidence matrix of the underlying graph

The best possible lower bound can be achieved when $\mathcal{B}_{n1,n2} = \mathcal{K}_{n/2,n/2}$ and the best possible upper bound is achieved when $\mathcal{B}_{n1,n2} = \mathcal{P}_n$.

V. Extending Consensus-based Approaches for Soft Robotics Applications

Soft robots composed of a homogeneous continuum of soft material can predict their own dynamics, which is an essential capability to have a lower-level sparse controller. In order to improve the performance of flexible robotic systems, we will adopt the machinery developed in the theoretical computer science community for graph sparsification and combine it with fractional calculus for nonlinear dynamics to find a sparse underlying topology.

The complex behaviour of visco-elastic materials can be approximated with classical Maxwell and Kevin-Voigt models, which dramatically limits model parameter estimation and optimal design mechanisms.

Since soft robots are entitled by visco-elastic property of porous media and long-term memory, these properties cannot be fully modelled using ordinary differential equations and instead modelled using fractional calculus.

The position and velocity of each node are governed by

$$\Sigma_i : \begin{cases} \dot{v}_i(t) \;=\; \frac{1}{m_i} u_i(t), \\ \dot{x}_i(t) \;=\; v_i(t), \end{cases} \tag{18}$$

where m_i is an inertia coefficient of node i, the position and the velocity of node i is obtained by $x_i(t)$ and $v_i(t)$, respectively. The feedback laws from the morphology depend on relative positions with respect to a subset of other nodes, a.k.a. nearest neighbors. We introduce a weighted graph $\mathcal{G} = (\mathcal{V}, \mathcal{E}, k)$ with n nodes and m links, where the vertices are masses of the complex soft network, and an edge between vertices is a springpot (i.e., a generalization of the classical visco-elastic elements). Then the incidence matrix $D_{n\times m}$ of the underlying graph G generates a vector of relative velocities y_e for the edges $e \in E$ by $y(t) = D^\top v(t)$, where $y^\top = [(y_1)^\top, \ldots, (y_n)^\top]^\top$ and $v^\top = [(v_1)^\top, \ldots, (v_n)^\top]^\top$. The coupling of the relative position dynamics is governed by

$$\Lambda_e : \begin{cases} \frac{d^\alpha}{dt^\alpha} z_e(t) \;=\; k_e(t) y_e(t) \;+\; \xi_e(t), \\ w_e(t) \;=\; z_e(t), \end{cases} \tag{19}$$

where k_e is the parameter of link e and $\xi(t)$ is measurement noise on link e. These coupling dynamics (Λ_e) are a generalization of the classical visco-elastic elements (both the spring and the dashpot) and present behavior that is intermediate between these two elements (see Fig. 4). Finally, vector $u(t) = Dw(t)$ is fed back to the nodes where D is the adjacency matrix of the morphology $\mathcal{G}$. The closed-loop dynamics of the network (19) with feedback control loops given by graph G (i.e., incidence matrix D) can be written in the following compact form

$$\begin{cases} \dot{v}(t) \;=\; -M^{-1} D z(t), \\ \frac{d^\alpha}{dt^\alpha} z(t) \;=\; K D^\top v(t) \;+\; \xi(t), \end{cases} \tag{20}$$

where M and K are diagonal matrices with m_i's and K_e's on their diagonals, respectively, and vector $z^\top = [(z_1)^\top, \ldots, (z_m)^\top]^\top$.

From (20), we get,

$$v(t) = E_{\gamma,1}(At^\gamma) v(0) + B.t^{\gamma-1} E_{\gamma,\gamma}(At^\gamma) * \xi_e(t), \tag{21}$$

where $\gamma = \alpha + 1$, $A = -M^{-1}DKD^\top$, $B = M^{-1}D$ and $E_{\gamma,1}$ is the Mittag Leffler function.

Example 2: Let us consider system (20) with 100 nodes over path graph $\mathcal{P}_{100}$. The initial velocity for the nodes are assumed to be $v_0 = [1, 2, 3, 4, \cdots, 100]$. The masses of all the nodes were assumed to be unity, and the spring constants, k_e's were assumed to be -1 for all the nodes. The network is then stimulated to reach consensus for various values of α, along with a Gaussian noise with mean 0, and standard deviation, $\sigma = 0.01$. Figs. 5 and 6 depict the velocity time graph and position time graph for $\alpha \in (0.5, 2)$. From Figs. 5 and 6, we can see that, as $\alpha \to 2$, the system becomes unstable and the position of the nodes tends to go to ∞. Additionally, Fig. 7 displays the position-time graph for the 100 nodes wherein the initial velocities of the nodes are assumed to be random, for $\alpha = 0.75$ and $\alpha = 0$, where a small perturbed Gaussian disturbance of standard deviation $\sigma = 0.01$, is being applied to the system. We can see that when $\alpha = 0$, i.e., for a first order system ($\gamma = \alpha + 1$, the order of the system, see (21)), reaching a consensus state is slower when compared to a fractional order system (see Fig. 7).

VI. Conclusions

This paper investigates the performance degradation of multi-agent networks under exogenous stochastic disturbances. To accurately model multi-agent systems with reduced parameters, we utilize the Virtual Viscoelastic-Based Model for inter-agent interaction in multi-agent networks via fractional-order systems. We employ Caputo derivatives and Laplace transforms to formulate fractional-order differential equations for the entire network dynamics and use the $\mathcal{H}_2$ norm as a performance measure. Through a graph-theoretic methodology, we relate the performance measure to the underlying graph's structural specifications and quantify fundamental limits on the best achievable levels of performance. Our analysis characterizes the tradeoffs between network

Unweighted Coupling Graph	Lower Bound	Upper Bound
Arbitrary	$\mathfrak{A}\ n^{-\beta}\ \ (n-1)$	$\mathfrak{A}\ 2^{-\beta}\ \sum_{k=1}^{n-1}\left(1-\cos(\frac{\pi k}{n})\right)^{-\beta}$
Tree	$\mathfrak{A}\ (n^{-\beta}+(n-2)^{-\beta-1}$	$\mathfrak{A}\ 2^{-\beta}\ \sum_{k=1}^{n-1}\left(1-\cos(\frac{\pi k}{n})\right)^{-\beta}$
Bi-partite	$\mathfrak{A}\ \left(\left(2\sqrt{\frac{Z(G)}{n}}\right)^{-\beta}+\frac{\left(2m-2\sqrt{\frac{\mathbf{Z(G)}}{n}}\right)^{-\beta}}{(n-2)^{-\beta-1}}\right)$	$\mathfrak{A}\ 2^{-\beta}\ \sum_{k=1}^{n-1}\left(1-\cos(\frac{\pi k}{n})\right)^{-\beta}$

TABLE I: Universal bounds on performance (14) for unweighted FLTI Consensus networks in G_n.

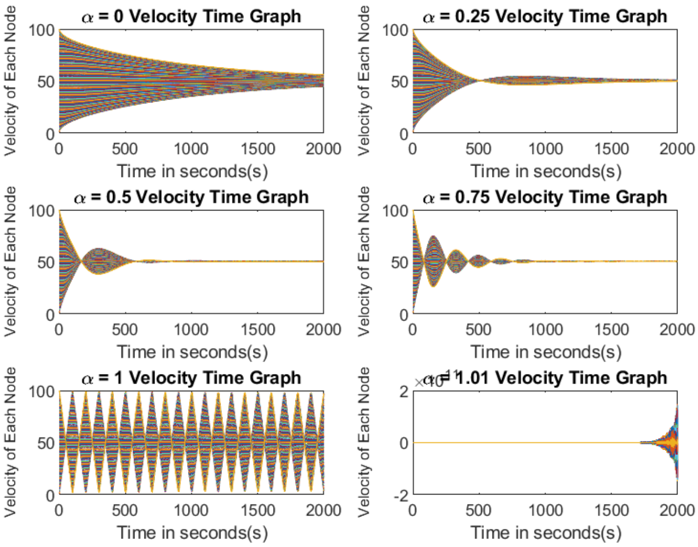

Fig. 5: Velocity-time plots for system (20) on a 100-node path graph, for $\alpha \in [0, 1.25]$ and Gaussian noise ($\sigma = 0.01$).

sparsity and performance measure and reveals their interplay. The findings highlight the impact of network topology on the performance of fractional-order consensus networks. To support the theoretical results, we provide numerical simulations that demonstrate the usefulness of our findings.

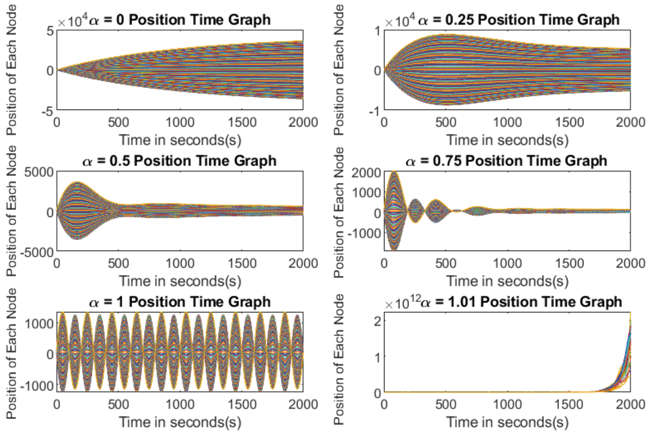

Fig. 6: Position-time plots for system (20) on a 100-node path graph, for $\alpha \in [0, 1.25]$ and Gaussian noise ($\sigma = 0.01$).

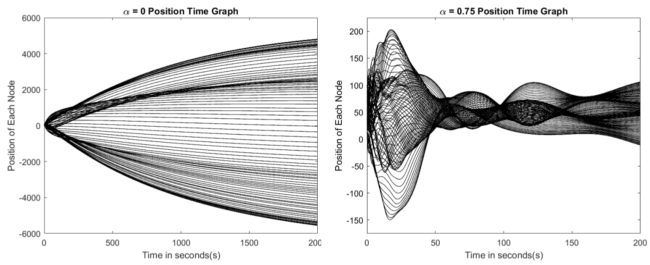

Fig. 7: Plots of position versus time for system (20) over the path graph with 100 nodes and Gaussian noise input with standard deviation $\sigma = 0.01$, for different values of $\alpha = 0$ and $\alpha = 0.75$.

REFERENCES

[1] P. M. Van den Hof, A. Dankers, P. S. Heuberger, and X. Bombois, "Identification of dynamic models in complex networks with prediction error methods—basic methods for consistent module estimates," *Automatica*, vol. 49, no. 10, pp. 2994–3006, 2013.

[2] T. Zhou, "On the controllability and observability of networked dynamic systems," *Automatica*, vol. 52, pp. 63–75, 2015.

[3] M. Siami and N. Motee, "Fundamental limits and tradeoffs on disturbance propagation in linear dynamical networks," *IEEE Transactions on Automatic Control*, vol. 61, no. 12, pp. 4055–4062, 2016.

[4] M. Siami and N. Motee, "New spectral bounds on h2-norm of linear dynamical networks," *Automatica*, vol. 80, pp. 305 – 312, 2017.

[5] M. Rahmani, A. Ghanbari, and M. M. Ettefagh, "Robust adaptive control of a bio-inspired robot manipulator using bat algorithm," *Expert Systems with Applications*, vol. 56, pp. 164–176, 2016.

[6] D. Rus and M. T. Tolley, "Design, fabrication and control of soft robots," *Nature*, vol. 521, no. 7553, pp. 467–475, 2015.

[7] Y. M. Efremov, T. Okajima, and A. Raman, "Measuring viscoelasticity of soft biological samples using atomic force microscopy," *Soft matter*, vol. 16, no. 1, pp. 64–81, 2020.

[8] O. Lieleg, K. Schmoller, M. M. Claessens, and A. Bausch, "Cytoskeletal polymer networks: viscoelastic properties are determined by the microscopic interaction potential of cross-links," *Biophysical journal*, vol. 96, no. 11, pp. 4725–4732, 2009.

[9] R. L. Magin, H. Karani, S. Wang, and Y. Liang, "Fractional order complexity model of the diffusion signal decay in mri," *Mathematics*, vol. 7, no. 4, p. 348, 2019.

[10] R. L. Bagley and P. J. Torvik, "Fractional calculus-a different approach to the analysis of viscoelastically damped structures," *AIAA journal*, vol. 21, no. 5, pp. 741–748, 1983.

[11] F. Mainardi, *Fractional calculus and waves in linear viscoelasticity: an introduction to mathematical models*. World Scientific, 2022.

[12] R. Caponetto, *Fractional order systems: modeling and control applications*, vol. 72. World Scientific, 2010.

[13] B. Bamieh, M. Jovanović, P. Mitra, and S. Patterson, "Coherence in large-scale networks: Dimension-dependent limitations of local feedback," *Automatic Control, IEEE Transactions on*, vol. 57, pp. 2235 –2249, Sept. 2012.

[14] R. Olfati-Saber and R. Murray, "Consensus problems in networks of agents with switching topology and time-delays," *Automatic Control, IEEE Transactions on*, vol. 49, pp. 1520–1533, Sept 2004.

[15] W. Dong, "Consensus of high-order nonlinear continuous-time systems with uncertainty and limited communication data rate," *IEEE Transactions on Automatic Control*, vol. 64, no. 5, pp. 2100–2107, 2018.

[16] A. Jadbabaie, J. Lin, and A. S. Morse, "Coordination of groups of mobile autonomous agents using nearest neighbor rules," *IEEE Transactions on automatic control*, vol. 48, no. 6, pp. 988–1001, 2003.

[17] M. Siami, "Stability and robustness analysis of commensurate fractional-order networks," *IEEE Transactions on Control of Network Systems*, vol. 8, no. 3, September, 2021.

[18] M. S. Tavazoei, M. Haeri, S. Jafari, S. Bolouki, and M. Siami, "Some applications of fractional calculus in suppression of chaotic oscillations," Nov 2008.

[19] M. S. Tavazoei, M. Haeri, M. Siami, and S. Bolouki, "Maximum number of frequencies in oscillations generated by fractional order lti systems," *IEEE Transactions on Signal Processing*, vol. 58, pp. 4003–4012, Aug 2010.

[20] M. Siami and M. S. Tavazoei, "Oscillations in fractional order lti systems: Harmonic analysis and further results," *Signal Processing*, vol. 93, no. 5, pp. 1243 – 1250, 2013.